JOURNAL OF SOLID STATE CHEMISTRY 67, 70–77 (1987)

The Crystal Structure of $CeRu_2B_2$ and Isotypic Compounds $M(Ru, Os)_2B_2$, M = La, Pr, Nd, Sm, Gd, and Th

C. HORVATH, P. ROGL, AND K. HIEBL

Institut für Physikalische Chemie der Universität Wien, Währingerstrasse 42, A-1090 Vienna, Austria

Received December 17, 1985; in revised form April 11, 1986

The crystal structure of $CeRu_2B_2$ has been determined from single-crystal X-ray counter data. The crystal structure of $CeRu_2B_2$ is closely related to the $CaRh_2B_2$-type structure. $CeRu_2B_2$ is face-centered orthorhombic with the lattice parameters: a = 6.4861(27), b = 9.0573(60), and c = 10.0263(27) Å, Z = 8. Due to small deviations from space group symmetry $Fddd$ (D_{2h}^{24}), the actual symmetry is $F222$ (D_2^7). The structure was solved by Patterson methods and refined by full matrix least-squares calculations. For an asymmetric set of 217 independent reflections ($|F_o| > 2\sigma(F_o)$), the obtained reliability factors were $R = \Sigma|\Delta F|/\Sigma|F_o| = 0.024$, $R_w = 0.020$ for the calculation in the higher symmetry space group $Fddd$. Isotypic compounds {RE, Th} {Ru, Os}$_2B_2$ have been synthesized with the light (ceric) rare-earth elements RE = La, Ce, Pr, Nd, Sm, and Gd and with thorium. The magnetic behavior of the cerium-containing borides Ce(Ru, Os)$_2B_2$ was studied in the temperature range from 1.6 to 1100 K. No superconductivity was observed. Practically no solubility was observed for silicon in $CeRu_2B_2$ and $CeOs_2B_2$ alloys (both as cast and annealed at 1100°C).

Introduction

A series of papers has been devoted in the past to the interesting and unusual properties of ternary borides containing cerium in combination with one of the metals of the platinum group (*1–5*). As part of our general programme concerning the constitution and thermodynamic phase equilibria, compound formation, and structural chemistry of ternary cerium–transition metal borides in respect to their magnetic and electric properties, we have recently focused on the alloy systems Ce–{Ru, Os}–B. New compounds $CeRuB_2$ with the $LuRuB_2$-type (*6*) and Ce(Ru, Os)$_2B_2$ have been synthesized; the crystallographic and thermomagnetic characterization of the latter phases as well as the possible formation of isotypic crystal structures in the homologous rare-earth systems became the subject of the present work.

Experimental

All compounds were prepared from commercially available high-purity elements: rare-earth metals (filings from ingots, 99.99%, Rare Earths Products Ltd., GB); ruthenium, osmium (powders: 99.9%, Engelhard Ind. Div., USA); thorium (powder, 99.9%, Cerac, USA), and boron (powder, crystalline, 99%, Koch Light Lbs., GB). The well blended mixtures with a nominal composition RE (20 at.%), T (40), B (40) of a total weight of 0.5–1 g each, were compacted in steel dies without the use of lubricants or binder materials. The compacted pellets were reacted in an arc melting furnace on a water-cooled copper

0022-4596/87 $3.00

hearth using a nonconsumable 2%-thoriated tungsten electrode in a Ti/Zr-gettered argon atmosphere. Weight losses due to the arc melting process were checked to be less than 1 wt%. A part of each alloy button was wrapped in Mo-foil, sealed in evacuated quartz tubes, annealed at 1000°C for 330 hr, and finally quenched in water.

From X-ray powder diffraction analysis the as-cast and annealed alloys generally were found to be multiphase and in some cases repeated annealing at higher temperatures (1400°C) in a tungsten sheet metal high-vacuum furnace proved necessary to reveal the new phase. Homogeneity of those alloys which were further investigated by magnetochemical techniques, was checked by metallography.

Precise lattice parameters and standard deviations were evaluated by a least-squares extrapolation method from room-temperature Guinier-Huber powder photographs using monochromatized Cu$K\alpha_1$ radiation and an internal standard of 99.9999% pure germanium (a_0 = 5.657906 Å). X-ray powder intensities were recorded by means of a KD-530 microdensitometer.

For the susceptibility measurements in the temperature range 80 < T < 1100 K a pendulum susceptibility meter (*7*) was employed, using a Faraday compensation method under He for T < 300 K, and under high-purity argon at T > 300 K.

The low-temperature susceptibility data (1.5 K < T < 80 K) were recorded on a Faraday-type Cahn electrobalance (*8*) with spectrosil quartz buckets under helium.

Superconductivity was checked using ac-induction equipment (*9*).

Results and Discussion

A. Determination of the Crystal Structure of $CeRu_2B_2$

To obtain single crystals, alloy buttons with a nominal composition Ce(28.5%), Ru(36.5), B(35.0) were annealed at 1000°C for 300 hr and quenched. A small single-crystal fragment with the dimensions 38 ×

TABLE 1

ATOMIC AND THERMAL PARAMETERS FOR $CeRu_2B_2$: COMPARISON OF PARAMETERS FOR REFINEMENT IN THE TWO DIFFERENT SPACE GROUPS, *Fddd* AND *F*222[a]

Atom	Site	x	y	z	Occ.	$U_{equ.}$ (Å²)	U_{11}	U_{22}	U_{33}	U_{12}
I. Space group $Fddd - D_{2h}^{24}$, No. 70; origin at $\bar{1}$, Z = 8; R = 0.024, R_w = 0.020										
Ce	8*a*	⅛	⅛	⅛	1.0	0.97	1.02(2)	0.87(2)	1.02(2)	—
Ru	16*g*	⅛	⅛	0.4886(1)	1.0	0.81	0.81(2)	0.89(2)	0.72(3)	−0.16(3)
B	16*f*	⅛	0.4432(9)	⅛	1.0	1.11	1.11(13)			
Correction for isotropic secondary extinction: 7.5(1.0) × 10^{-7}										
II. Space group $F222 - D_2^7$, No. 22; origin at 222, Z = 8; R = 0.021, R_w = 0.017										
Ce1	4*a*	0	0	0	1.0	1.29	1.57(12)	1.68(14)	0.62(14)	—
Ce2	4*c*	¼	¼	¼	1.0	0.74	0.56(9)	0.24(8)	1.43(15)	—
Ru1	8*g*	0	0	0.3627(3)	1.0	0.98	0.73(11)	0.31(14)	0.90(17)	0.17(10)
Ru2	8*h*	¾	¼	0.3856(3)	1.0	0.68	0.92(11)	0.57(10)	0.55(14)	0.05(9)
B1	8*f*	0	0.3134(39)	0	1.0	1.27	1.27(67)			
B2	8*i*	¾	0.0719(32)	¼	1.0	0.96	0.96(62)			
Correction for isotropic secondary extinction: 6.8(9) × 10^{-7}										

[a] Crystallographic data are: a = 6.4861(27), b = 9.0573(60), c = 10.0263(27) Å, V = 589.01(50) Å³, D_x = 8.22 Mgm^{-3} and μ(Mo$K\alpha$) = 23.4 mm^{-1}. Standard deviations are in parenthesis; isotropic temperature factors are expressed as $T = \exp[-2\pi^2 \times 10^{-2} U(2 \sin\theta/\lambda)^2]$; anisotropic thermal factors are of the form $T = \exp[-2\pi^2 \times 10^{-2}(U_{11}h^2a^{*2} + U_{22}k^2b^{*2} + U_{33}l^2c^{*2} + 2U_{12}hka^*b^* + \cdots)]$; by symmetry $U_{13} = U_{23} = 0$.

45 × 70 μm was obtained by mechanical fragmentation. Weissenberg photographs along the needle axis [100] first revealed an A-centered monoclinic cell with the lattice dimensions $a = 5.9746(10)$, $b = 9.0524(63)$, $c = 6.4845(12)$ Å and $\beta = 122.95(1)°$. Reduction of the unit cell and transformation of the axes, however, resulted in an overall face-centered orthorhombic lattice (see Table I). After reorientation of the crystal fragment along the orthorhombic [100] axis a complete set of oscillation and Weissenberg photographs were taken, essentially consistent with space group symmetry *Fddd*. Reflections (0*kl*), (*h*0*l*) and (*hk*0) were practically unobserved for $k + l = 4n$, $h + l = 4n$, or $h + k = 4n$; the very few exceptions, i.e., the low-intensity reflections (020), (240), (420), etc., however, reveal small deviations from the higher symmetry violating the condition for the existence of diagonal glide planes in *Fddd*; the actual space group thus is *Fmmm*, *Fmm*2 or the direct crystallographic subgroup *F*222.

Integrated intensities were collected up to a limit of $\sin\theta/\lambda = 0.85$ Å^{-1} on an automatic STOE-four circle diffractometer using monochromatized Mo*Kα* radiation. A set of 269 symmetry-independent reflections was obtained by averaging "centered reflections" out of a total number of 874 recorded intensity data, and all observed intensities (217 for $|F_0| > 2\sigma$) were used in the structure refinement. An empirical absorption correction was applied using psi-scans of two independent reflections. Cell parameters were evaluated in a least-squares refinement procedure from the 2θ values of 12 higher order reflections. The crystallographic data are listed in Table I.

Comparison of the atom volumes with the volume of the unit cell and assuming a space filling of ca. 70% resulted in a cell content of 8 formula units $CeRu_2B_2$. A three-dimensional Patterson map $P(u, v, w)$ was found to be consistent with a structure model based on the $CaRh_2B_2$ structure (*10*). As a statistical test for a center of symmetry turned out to be inconclusive, the structure model was first refined in the higher symmetry space group *Fddd* using the STRUCSY full matrix least-squares program system (STOE & Cie., Darmstadt, FRG). The weights used were based upon counting statistics $w_i = 1/(\sigma(F_i))^2$, and structure factors were furthermore corrected for isotropic secondary extinction. The crystallographic sites of the boron atoms (16 B in 16*f*) were clearly resolved from a Fourier difference map $F_o - F_{Ce,Ru}$. Refinement of the occupancies of the metal atoms did not result in a significant deviation from full occupation. At this point a difference map

TABLE II

INTERATOMIC DISTANCES IN $CeRu_2B_2$ (<4 Å)[a]

I. Space group *Fddd* – D_{2h}^{24} (origin $\bar{1}$)							
Ce	–4 Ce	3.747(1)	Ru	–2 Ce	3.009(1)	B	–1 Ce	2.882(8)
				–2 Ce	3.520(1)		–2 Ce	3.049(2)
	–4 Ru	3.009(1)		–1 Ce	3.646(1)		–2 Ce	3.637(4)
	–4 Ru	3.520(1)						
	–2 Ru	3.646(1)		–1 Ru	2.735(2)		–2 Ru	2.076(3)
				–2 Ru	2.794(1)		–2 Ru	2.141(6)
	–2 B	2.882(8)		–4 Ru	3.747(1)			
	–4 B	3.049(2)		–2 Ru	3.963(1)			
	–4 B	3.637(4)						
				–2 B	2.076(3)			
				–2 B	2.141(6)			
II. Space group *F*222 – D_2^7								
Ce1	–4 Ce2	3.747(1)	Ru1	–2 Ce2	3.006(2)	B1	–1 Ce1	2.839(35)
				–2 Ce1	3.523(2)		–2 Ce2	3.040(7)
	–4 Ru2	3.012(2)		–1 Ce1	3.637(3)		–2 Ce1	3.657(16)
	–4 Ru1	3.523(2)						
	–2 Ru1	3.637(3)		–1 Ru1	2.753(4)		–2 Ru2	2.068(10)
				–2 Ru2	2.795(1)		–2 Ru1	2.180(28)
	–2 B1	2.839(35)		–2 Ru2	3.736(3)			
	–4 B2	3.056(6)		–2 Ru2	3.758(3)			
	–4 B1	3.657(16)		–2 Ru1	3.953(3)			
				–2 B2	2.081(9)			
				–2 B1	2.180(28)			
Ce2	–4 Ce1	3.747(1)	Ru2	–2 Ce1	3.012(2)	B2	–1 Ce2	2.916(29)
				–2 Ce2	3.517(2)		–2 Ce1	3.056(6)
	–4 Ru1	3.006(2)		–1 Ce2	3.654(3)		–2 Ce2	3.622(13)
	–4 Ru2	3.517(2)						
	–2 Ru2	3.654(3)		–1 Ru2	2.719(4)		–2 Ru1	2.081(9)
				–2 Ru1	2.795(1)		–2 Ru2	2.110(22)
	–2 B2	2.916(29)		–2 Ru1	3.736(3)			
	–4 B1	3.040(7)		–2 Ru1	3.758(3)			
	–4 B2	3.622(13)		–2 Ru2	3.972(3)			
				–2 B1	2.068(10)			
				–2 B2	2.110(22)			

[a] The B—B distances are >3 Å and are not listed.

$F_o - F_c$ was featureless; the obtained reliability values were $R = 0.024$ ($R_w = 0.020$).

To account for the small symmetry deviations the structure model was transferred into the noncentrosymmetric crystallographic subgroup $F222$ (D_2^7-No. 22) and refined to $R = 0.021$, $R_w = 0.017$ (the structure model does not comply with the space groups *Fmmm* or *Fmm*2). The decrease in the residual values with respect to the refinement in *Fddd*, however, is rather small, consistent with the rather minute deviations from centrosymmetry. The final positional and thermal parameters for both refinements are summarized in Table I and atomic distances up to a limit of 4 Å are shown in Table II; a table comparing the calculated (F222) and observed structure factors is available on request from the authors.

Using the single-crystal atom parameters excellent agreement was found between calculated and observed powder diffraction intensities. Deviations from the *Fddd* symmetry are by far not intense enough to be discernible from X-ray powder data.

B. Isotypic Borides (RE, Th)Ru_2B_2 and (RE, Th)Os_2B_2, RE = La, Ce, Pr, Nd, Sm, and Gd

X-ray powder diffractometric analysis of (RE, Th) (Ru, Os)$_2B_2$ alloys arc melted and annealed at 1000°C confirmed the existence of a new compound for the early (ceric) rare-earth members RE = La, Ce, Pr, Nd, Sm, Gd and for thorium. Guinier photographs of the new compounds show a striking similarity with the powder diffractogram of $CeRu_2B_2$ and are all indexed on the basis of an overall face-centered orthorhombic unit cell (see Table III). Composition, unit cell dimensions and X-ray powder intensity data indicate structural analogy with the structure type of $CeRu_2B_2$ or $CaRh_2B_2$. Using the atom parameters as derived from the $CeRu_2B_2$ single-crystal data, calculated and observed powder intensities were found to be in fine agreement for both series of compounds (RE, Th) Ru_2B_2 and (RE, Th)Os_2B_2 and for RE = La, Ce, Pr, Nd, Sm, Gd. The details of the powder diagram of $PrOs_2B_2$ are presented in Table IV; for a complete information the observed X-ray powder intensities are compared with those calculated in $F222$ symmetry using the atom parameters derived for $CeRu_2B_2$.

C. Solubility of Silicon in $CeRu_2B_2$ and $CeOs_2B_2$

X-ray powder analysis of alloys $CeRu_2B_{2-x}Si_x$ and $CeOs_2B_{2-x}Si_x$ essentially revealed a two-phase structure. In both alloy series the solubility of Si in $CeRu_2B_2$ and $CeOs_2B_2$, respectively, appears to be rather limited; there is practically no homogeneous range observed and no change in the unit cell dimensions of Ce(Ru, Os)$_2B_2$. From two-phase alloys annealed at 1000°C the following data were obtained: $CeRu_2B_{1.5}Si_{0.5}$: $a = 6.4782(41)$, $b = 9.0566(92)$, $c = 10.0259(20)$ Å, $V = 588.23(72)$ Å^3 and for $CeOs_2B_{1.5}Si_{0.5}$: $a = 6.5620(24)$, $b = 9.0606(72)$, $c = 10.0435(17)$ Å and $V = 597.15(53)$ Å^3. The two-phase microstructure therefore consists of practically ter-

TABLE III

CRYSTALLOGRAPHIC DATA OF THE TERNARY BORIDES (RE, Th) (Ru, Os)$_2B_2$

Compound	Lattice parameters (Å)			
	a	*b*	*c*	*V*
$LaRu_2B_2$	6.4369(24)	9.2159(32)	10.1600(16)	602.71(32)
$CeRu_2B_2$	6.4793(19)	9.0562(58)	10.0259(14)	588.31(42)
$PrRu_2B_2$	6.4715(29)	9.1117(79)	10.0193(17)	590.81(58)
$NdRu_2B_2$	6.4807(32)	9.0854(36)	9.9753(15)	587.34(39)
$SmRu_2B_2$	6.5081(18)	9.0275(40)	9.8803(21)	580.49(33)
$GdRu_2B_2$	6.5291(41)	8.9916(61)	9.8033(21)	575.53(54)
$ThRu_2B_2$	6.4608(17)	9.0759(20)	10.0927(25)	591.81(25)
$LaOs_2B_2$	6.5159(34)	9.2152(89)	10.2105(28)	614.09(69)
$CeOs_2B_2$	6.5574(30)	9.0599(45)	10.0430(17)	596.65(42)
$PrOs_2B_2$	6.5496(23)	9.1089(41)	10.0700(49)	600.78(45)
$NdOs_2B_2$	6.5622(39)	9.0824(41)	10.0229(19)	597.37(46)
$SmOs_2B_2$	6.5847(29)	9.0266(50)	9.9413(20)	590.88(43)
$GdOs_2B_2$	6.6175(31)	8.9917(60)	9.8608(24)	586.75(50)
$ThOs_2B_2$	6.5169(11)	9.1269(14)	10.1340(16)	602.76(17)

TABLE IV

POWDER DIFFRACTION DATA FOR $PrOs_2B_2$[a]

	$\sin^2\theta \times 10^4$		Intensity			$\sin^2\theta \times 10^4$		Intensity	
(*hkl*)	Obs.	Calc.	Obs.	Calc.	(*hkl*)	Obs.	Calc.	Obs.	Calc.
(200)	*	234	*	0.0	(604)	*	3251	*	0.0
(111)	268	268	23	19.3	(533)	3355	3351	24	6.2
(002)	*	286	*	0.0	(044)		3357		17.0
(202)	520	520	4	4.7	(226)	*	3362	*	0.0
(020)	*	553	*	0.0	(515)	3388	3389	5	5.2
(311)	736	736	94	94.5	(442)	*	3435	*	0.0
(220)	790	787	6	5.1	(406)	*	3511	*	0.0
(022)	840	839	103	100.0	(335)	3558	3559	10	12.1
(113)		840		2.8	(151)	*	3588	*	0.8
(400)	936	936	8	6.6	(244)	*	3591	*	0.0
(222)	*	1073	*	0.0	(713)	3647	3649	3	2.5
(004)	1145	1144	34	34.2	(117)	*	3701	*	0.7
(402)	*	1222	*	0.0	(800)	3744	3745	8	6.5
(313)	1306	1309	50	48.1	(624)	3803	3804	11	10.2
(131)	1377	1375	2	2.4	(802)	*	4031	*	0.0
(204)	*	1378	*	0.0	(351)	4056	4056	12	11.4
(420)	*	1489	*	0.0	(426)	4065	4064	5	4.9
(511)	1673	1673	12	13.1	(153)	*	4160	*	0.5
(024)	*	1697	*	0.0	(317)	4168	4169	10	11.6
(422)	1776	1775	13	14.6	(713)	4183	4183	2	2.8
(331)	1843	1843	29	27.5	(444)	4297	4293	6	5.3
(224)	1932	1931	2	2.0	(820)	*	4298	*	0.0
(133)	*	1947	*	1.0	(640)	*	4319	*	0.0
(115)	*	1985	*	1.7	(535)	4498	4495	4	4.4
(404)	2081	2080	5	5.5	(008)	4585	4577	30	6.9
(600)	*	2106	*	0.0	(822)		4584		21.7
(040)	2212	2213	12	14.8	(642)	4609	4605	10	9.1
(531)	2244	2245	9	10.0	(353)	4626	4628	11	12.0
(602)	2393	2392	7	8.0	(606)	4682	4681	4	5.2
(333)	2414	2415	19	20.8	(733)	*	4755	*	2.3
(240)	*	2447	*	0.0	(046)	*	4787	*	0.0
(315)	2453	2453	19	18.3	(715)	*	4793	*	2.9
(042)	*	2499	*	0.0	(137)	*	4807	*	0.6
(006)	*	2574	*	0.0	(208)	*	4811	*	0.0
(424)	*	2634	*	0.0	(804)	4890	4889	10	11.4
(620)	2659	2660	10	8.1	(911)	*	4949	*	0.4
(242)	*	2733	*	1.1	(060)	*	4979	*	0.0
(531)	2780	2779	8	6.7	(551)	4991	4992	3	4.8
(206)	*	2808	*	0.8	(246)	*	5021	*	1.2
(622)	*	2946	*	0.0	(517)	5106	5105	4	5.1
(711)	3076	3077	4	3.6	(028)	*	5130	*	0.0
(135)	*	3091	*	1.0	(260)	*	5213	*	0.6
(062)	3129	3128	18	19.2	(626)	*	5234	*	0.0
(440)	*	3149	*	2.9	(062)	5265	5265	17	15.0

[a] *Material*: Pr(20)Os(40)B(40), annealed at 1000°C (340 hr), quenched. *Method*: Powder diffraction in a Guinier-camera (99.9999% Ge-standard). Lattice parameters are $a = 6.5496(23)$, $b = 9.1089(41)$, and $c = 10.0700(49)$ Å. Intensities calculated with atomic parameters as derived for $CeRu_2B_2$; $R_I = 0.097$. $I = mF^2 (1 + \cos^2 2\theta)/\sin^2\theta \cos\theta$ is normalized to the strongest reflexion, $I = 100$.

nary Ce(Ru, Os)$_2B_2$ in thermodynamic equilibrium with the $ThCr_2Si_2$-type counter solution phases $CeRu_2Si_{2-x}B_x$ and $CeOs_2Si_{2-x}B_x$, respectively; for details see also Ref. (*11*).

D. Crystal Chemistry

A plot of the lattice parameters vs. the lanthanide atomic number (Z) for the RE (Ru, Os)$_2B_2$ phases is shown in Fig. 1. The plots of b, c and of the volume vs Z show the typical lanthanide contraction. The a parameter, however, varies in the opposite manner showing an unusual expansion.

The structural chemistry of the $CaRh_2B_2$-type and its close relation to the $CeCo_3B_2$-type was earlier discussed by (*10*), and there is a rather large variety of structure variants among ternary metal borides all deriving from the $CaCu_5$($CeCo_3B_2$)-type of structure, i.e., $HfCo_3B_2$, $REIr_3B_2$, $Nd_{0.71}Rh_{3.29}B_2$, $Li_{1.2}Ni_{2.5}B_2$, $Ba_2Ni_9B_6$, etc. (for a complete listing see Ref. (*14*)). All these structure types are characterized by the formation of 3.6.3.6 transition metal kagomé nets, directly stacked in layers along the c axis. For the $CaRh_2B_2$- and $RERu_2B_2$-type borides the problem of accomodating the large alkaline-earth atoms (or rare-earth atoms) is solved by the formation of defects within the puckered Rh(Ru) 3.6.3.6 layers thus forming Rh(Ru) chains, which introduce a high degree of anisotropy. In direction of the c axis the layers are shifted with respect to each other, thereby providing a rather dense packing of the structure. Boron atoms are isolated and are coordinated by four Rh(Ru) and five remote rare-earth atoms. The high anisotropy of the orthorhombic $CeRu_2B_2$ structure is reflected in the ratio $c/a \sim 1.5$ which strongly deviates from the ideal value of $\sqrt{3}$ and likely also accounts for the unusual expansion of the a axis mentioned above.

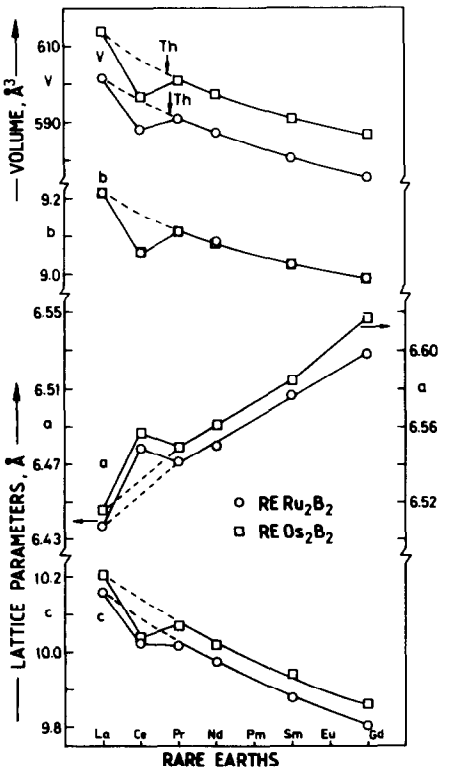

FIG. 1. Lattice parameters and volumes of (RE, Th) (Ru, Os)$_2B_2$ borides versus lanthanide atomic number.

E. Magnetic Behavior of Ce(Ru, Os)$_2B_2$

The inverse magnetic susceptibilities of Ce(Ru, Os)$_2B_2$ versus temperature are shown in Fig. 2. Attempts to interprete the high temperature data ($T > 200$ K) according to a simple Curie-Weiss law resulted in rather reduced effective magnetic moments with large negative paramagnetic Curie-temperatures ($CeRu_2B_2$, $\mu_{eff} = 2.0\ \mu_B$, $\theta_p = -311$ K; $CeOs_2B_2$, $\mu_{eff} = 1.7\ \mu_B$, $\theta_p = -260$ K). Upon lowering the temperature below 200 K we observe a significant reduction in the rate of decrease of χ_g^{-1} (T). This behavior is commonly attributed to the demagnetizing effects of spin fluctuations arising from Ce valence fluctuations. The variables, i.e., the spin fluctuation temperature, T_{SF}, and the excitation energy $E_{EX} = E(Ce^{3+}) - E(Ce^{4+})$, were refined by a least-

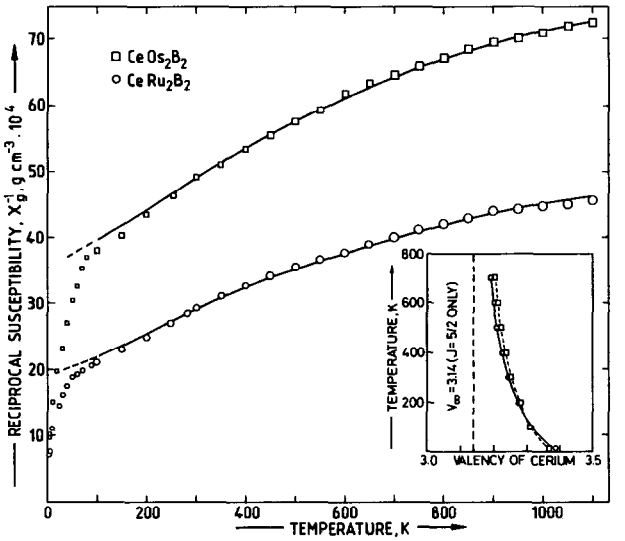

FIG. 2. Reciprocal gram susceptibility versus temperature for $CeRu_2B_2$, $CeOs_2B_2$, and calculated least-squares fit (solid line); the valency of cerium (calculated) is shown in the inset.

squares procedure according to the Ansatz based on the ICF model by Sales and Wohlleben (*12*) (for details see also (*13*)). Thus we arrive at $T_{SF} = -300$ K, $E_{EX} = 290$ cm^{-1} for $CeRu_2B_2$, and $T_{SF} = -400$ K, $E_{EX} = 340$ cm^{-1} for $CeOs_2B_2$. From these data the valency function $v(T)$ (see inset, Fig. 2) was calculated. The very sharp decrease of χ_g^{-1} below 50 K is mainly due to small amounts of stable moment Ce^{3+} contaminants (less than 3%), eventually including small amounts of secondary phases. These impurity contributions were subtracted prior to refinement. The partial B/Si exchange did not significantly alter the magnetism of the boride phases.

Acknowledgments

This investigation was supported by the Austrian Science Foundation (Fonds zur Förderung der wissenschaftlichen Forschung in Österreich) through Grant P5648 and by the U.S. Air Force Office of Scientific Research through Grant 80-0009. It was assisted in part by the NSF and the Materials Science Center at Cornell University. The single-crystal data collection was carried out on a STOE-four circle diffractometer of the Mineralogical Institute of the University of Vienna. We kindly thank Dr. F. Pertlik for technical assistance. P. R. expresses his gratitude to the Hochschuljubiläumsstiftung der Stadt Wien for the KD-530 type microdensitometer and the MNT-306 microbalance. The authors furthermore express their gratitude to the late Professor M. J. Sienko for his continuous interest in this work.

References

1. S. K. MALIK, A. M. UMARJI, G. K. SHENOY, P. A. MONTANO, AND M. E. REEVES, *Phys. Rev. B* **31**, 4728 (1985).
2. K. N. YANG, M. S. TORIKACHVILI, M. B. MAPLE, AND H. C. KU, *J. Appl. Phys.* **57**, 3140 (1985).
3. M. B. MAPLE, S. E. LAMBERT, M. S. TORIKACHVILI, K. N. YANG, J. W. ALLEN, B. B. PATE, AND I. LINDAU, *J. Less-Common Met.* **111**, 239 (1985).
4. S. K. MALIK, A. M. UMARJI, G. K. SHENOY, T. A. ALDRED, AND D. G. NIARCHOS, *J. Appl. Phys.* **57**, 3043 (1985).
5. K. HIEBL, P. ROGL, AND M. J. SIENKO, *Inorg. Chem.* **21**, 1128 (1982).
6. C. HORVATH AND P. ROGL, *Mater. Res. Bull.* **20**, 1273 (1985).
7. SUS-10 Susceptibility Measuring Device, A. Paar-KG., Graz, Austria.
8. J. E. YOUNG, JR., Ph.D. Thesis, Cornell University, 1971.

9. W. G. FISHER, Ph.D. Thesis, Cornell University, 1978.
10. B. SCHMIDT AND W. JUNG, *Z. Naturforschung B* **33,** 1430 (1978).
11. K. HIEBL, C. HORVATH, AND P. ROGL, *J. Less-Common Met.* **117,** 375 (1986).
12. B. C. SALES AND D. K. WOHLLEBEN, *Phys. Rev. Lett.* **35,** 1240 (1975).
13. K. HIEBL, C. HORVATH, P. ROGL, AND M. J. SIENKO, *Z. Phys. B* **56,** 201 (1984).
14. P. ROGL, *J. Less-Common Met.* **110,** 285 (1985).